PHASE FIELD MODELLING OF TWINNED DENDRITE GROWTH

M.A. Salgado-Ordorica, J.-L. Desbiolles and M. Rappaz

Computational Materials Laboratory, Ecole Polytechnique Fédérale de Lausanne
CH-1015 Lausanne, Switzerland
mario.salgado@epfl.ch, jean-luc.desbiolles@epfl.ch michel.rappaz@epfl.ch

Keywords: Directional solidification, Phase Field, Dendrite morphology, Wetting angle, Twin boundary

Abstract

Twinned dendrite growth has been found to occur in aluminum alloys when critical thermal conditions ($G \approx 100$ K/cm, $v_s \approx 1$ mm/s) and a slight convection in the melt are present during directional solidification. Split in their trunk by a coherent (111) twin plane, such dendrites grow along $\langle 110 \rangle$ directions with a complex branch structure of $\langle 110 \rangle$, but also sometimes $\langle 100 \rangle$ secondary arms. To explain the twinned dendrite growth kinetics advantage, Eady and Hogan suggested that the Young Laplace equation involving the solid-liquid interfacial energy γ_{sl} and the twin energy γ_t at the triple junction stabilizes a grooved tip(1). Wood et al proposed instead that torque terms associated with the anisotropy of $\gamma_{s\ell}$ stabilize a sharp pointed tip(2). Finally, Henry suggested the possibility of the existence of a doublon, initiated precisely by a grooved tip, that would evolve depending on the solute content(3). In a recent experimental work, we have shown that the doublon conjecture is probably not valid for high solute content aluminum alloys, whereas it could be valid at low composition. In the present work, the twinned dendrite tip morphology and growth kinetics have been investigated using a 3D phase field method implemented on a massively parallel computer. The twin boundary energy has been imposed via an appropriate boundary condition fixing the angle of the phase field gradient with respect to the boundary. Besides this angle, various experimental conditions such as thermal gradient, gradient direction, velocity of the isotherms and compositions have been investigated. The growth kinetics obtained under such conditions has been compared with that of regular dendrites.

Introduction

Feathery grains are often found as defects in semi-continuously cast billets or slabs of aluminum alloys (4; 5). They are made of $\langle 110 \rangle$ dendrite trunks split in their centre by a (111) twin plane, with $\langle 110 \rangle$, but also sometimes $\langle 100 \rangle$ side arms(6). Experience has shown that such structures nucleate and grow under relatively high thermal gradient and solidification speed ($G \approx 100$ K/cm and $v_s \approx 1$ mm/s), when some convection is present in the melt (7). Despite the fact that the alternated sequence of twinned and untwined regions appears progressively misoriented with respect to G, twinned dendrites clearly have a growth kinetic advantage over ordinary columnar dendrites. It has been suggested that this is due to two phenomena: the difference in dendrite tip morphology and solutal interactions between regular and twinned dendrites.
In terms of dendrite tip shape, Eady and Hogan(1) first proposed the existence of a groove at the dendrite tip that is stabilized by the Young-Laplace equation:

$$2\gamma_{s\ell} \cos\theta - \gamma_t = 0 \tag{1}$$

where $\gamma_{s\ell}$ is the solid-liquid interfacial energy, θ is the angle formed by the groove with respect to the twin plane and γ_t is the twin boundary energy. This schematic shape is shown in Fig. 1a, with the equilibrium condition at the triple junction. The interfacial energy related to the coherent twin boundary at the center of the dendrite trunk promotes the formation of a cusp at the dendrite tip. However, this simple two dimensional representation does not take into account the second main curvature radius of the tip (i.e. the three dimensional component of the system) or the anisotropy of $\gamma_{s\ell}$.

Wood et al(2) modified Lu and Hunt's model for dendritic solidification(8) by imposing a fixed angle between the dendrite tip and the twin plane. From their simulation results, it was concluded that an edgy or sharp dendrite was more advantageous in terms of solute segregation and growth undercooling with respect to regular dendrites having a dendrite tip with a larger radius of curvature. This situation is shown in Fig. 1b. Their predictions implied that twinned dendrites were supposed to grow under relatively low thermal gradient, which is not supported by experimental evidence. Moreover, an edgy dendrite tip requires to consider torque terms in the mechanical equilibrium condition at the triple junction. In order to make these terms sufficiently large, the solid-liquid interfacial energy anisotropy must be large too. However, it has been shown recently that it is actually very low in Al alloys, typically $\approx 1\%$ (9; 10). Even though this anisotropy could be slightly increased by the addition of solute elements such as Zn or Mg(11; 12), an edgy tip would not satisfy the equilibrium conditions in such alloys.

Finally, a doublon morphology was conjectured by Henry(3) based on experimental observations made in dilute industrial alloys. As can be seen in Fig. 1c, a doublon is a double dendrite tip that grows with a thin liquid channel, a few microns wide, in its center. It would be initiated by the small groove necessary to accommodate the twin energy, like in Eady and Hogan's hypothesis. Under equilibrium conditions, this liquid channel would see its composition increase with a temperature decrease (for $k_0 < 1$, where k_0 is the partition coefficient), and eventually, solidify near the solidus temperature, with a final liquid composition close to c_0/k_0, where c_0 is the nominal composition. The doublon conjecture was supported mainly by two experimental evidences: (i) in a section parallel to the twin plane, no secondary arms were clearly observed and growth seemed to be cellular rather than dendritic. The in-plane spacing $\lambda_{//}$ of these cellular trunks was much smaller than the distance $\lambda_\perp$ separating two successive rows of twinned dendrite trunks(3); (ii) using High Resolution Transmission Electron Microscopy (HRTEM), the solute composition in a region close to the twin plane was measured to be close to c_0 for an Al-4.3wt.% Cu-0.3wt.% Mg alloy.

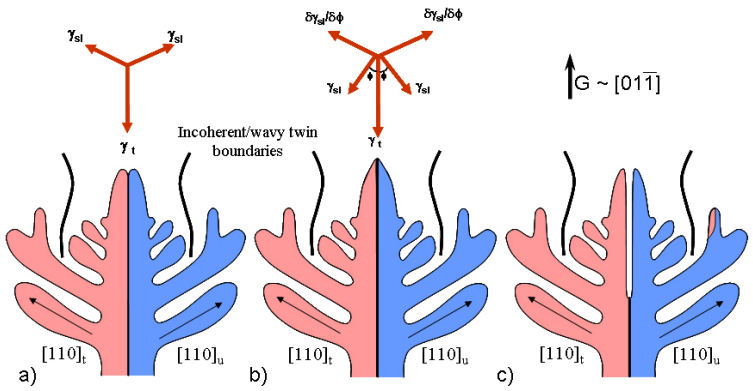

Figure 1: Schematic view of twinned dendrite tip morphologies according to Eady and Hogan(1) (a), Wood and Hunt(2) (b) and Henry(3) (c).

In a recent investigation, however, Salgado-Ordorica and Rappaz(6) showed that, for higher solute-content binary aluminum alloys, the primary spacings $\lambda_{//}$ and $\lambda_{\perp}$ were about the same with well developed dendrite side arms within the twin plane and away from it. Furthermore, no clear solute segregation at the dendrites trunk center was measured. In summary, if the edgy twinned dendrite tip can certainly be ruled out, a grooved or doublon type dendrite tip, whose depth might depend on the solute nature and content, are still two possible morphologies.

The objective of the present work is then to correlate these somewhat contradictory experimental observations with numerical simulations reproducing the physical conditions under which twinned dendrites are supposed to grow. The phase field method, which has been widely used over the last ten years in order to study the solidification of metallic alloys (13; 14; 15), has been chosen for this study. Its main advantage resides in the fact that the liquid-solid interface does not need to be tracked during solidification. Instead, a fixed and regular mesh is defined and a scalar variable, the phase field ϕ, describes the transition from one phase to the other. Such a method has been implemented onto a massively parallel computer and the boundary conditions as well as the thermophysical properties of the alloy have been adapted so as to reproduce the growth of half of a twinned dendrite with a mirror symmetry with its untwined counterpart.

Phase field model

A phase field model similar to the one described by Boettinger et al(13) has been implemented. The free energy functional F of the considered domain V is given by:

$$F = \int_V \left(f(T, c, \phi) + \frac{\varepsilon^2}{2} |\nabla \phi|^2 \right) dV \tag{2}$$

where f is the volumetric local free energy, function of temperature T, solute c and phase field ϕ. This parameter defines the solid and the liquid and varies continuously from $\phi = 1$ in the liquid to $\phi = 0$ in the solid. The parameter ε, together with a parameter W of a double well potential entering into f, define the solid-liquid interface energy $\gamma_{s\ell}$, and thickness δ. The thickness of the diffuse interface needs to be artificially enhanced to match the capabilities of nowadays computer for calculations relevant to 3D dendrite solidification. Instead of a few nanometers, which would be a realistic value for metallic alloys, δ is set to values in the range of $0.1 - 1$ μm (16). The anisotropy of $\gamma_{s\ell}$ is introduced via the parameter ε as:

$$\varepsilon(\vec{n}) = \bar{\varepsilon}\eta(\vec{n}) \tag{3}$$

where $\vec{n} = (n_x, n_y, n_z)$ is the unit vector normal to the interface in the crystallographic reference frame, and η is a function that describes the orientation dependence of $\gamma_{s\ell}$. For materials with a cubic structure, the equivalent form of the spherical harmonics that respect the cubic symmetry can be written as(15; 17):

$$\eta(\vec{n}) = 1 + \epsilon_4(Q - 3/5) + \epsilon_6(3Q + 66S - 17/7) + \epsilon_8(65Q^2 - 94Q - 208S + 33) \tag{4}$$

with $Q = n_x^4 + n_y^4 + n_z^4$ and $S = n_x^2 n_y^2 n_z^2$. The anisotropy coefficients ϵ_4, ϵ_6, ϵ_8 that appear in eq. 4 can induce various dendrite growth directions (higher order terms are not considered). For $\epsilon_4 > 0$ and $\epsilon_6 = \epsilon_8 = 0$, the normal $\langle 100 \rangle$ directions are selected. For $\epsilon_4 = \epsilon_8 = 0$ and $\epsilon_6 < 0$, dendrites grow along $\langle 110 \rangle$(3). For mixed values, e.g., $\epsilon_4 \neq 0$, $\epsilon_6 \neq 0$ and $\epsilon_8 = 0$, it has been shown recently that $\langle hk0 \rangle$ growth directions can vary from $\langle 100 \rangle$ to $\langle 110 \rangle$ depending

on the strength of the coefficients (11). The phase equation that describes the evolution of ϕ is given by the functional derivative of F, i.e.(13):

$$\frac{\delta\phi}{\delta t} = -M_\phi \frac{\delta F}{\delta \phi} = -M_\phi \frac{\partial f}{\partial \phi} - \vec{\nabla} \cdot (\varepsilon^2 \vec{\nabla}\phi) + \vec{\nabla} \cdot \left|\vec{\nabla}\phi\right|^2 \varepsilon \frac{\partial \varepsilon}{\partial(\vec{\nabla}\phi)} \tag{5}$$

where M_ϕ is equivalent to an interface kinetic coefficient. The solute diffusion equation is given by:(18)

$$\frac{\partial c}{\partial t} = \vec{\nabla} \cdot \left[\bar{D} \left(\vec{\nabla} c + \frac{(1-k_0)c}{\phi + k_0(1-\phi)} \vec{\nabla}\phi \right) \right] \tag{6}$$

with

$$c_l = \frac{c}{\phi + k_0(1-\phi)} \text{ and } \bar{D} = D_s + \frac{\phi}{\phi + k_0(1-\phi)}(D_l - D_s) \tag{7}$$

where c_l is the liquid composition, c the average composition ($c = \phi c_l + (1-\phi)c_s$), D_l and D_s are the diffusion coefficients in the liquid and the solid, respectively, and $\bar{D}$ is an average diffusion coefficient in the diffuse interface thickness.

In order to model the growth of twinned dendrites, some considerations have to be made. As stated before, these dendrites are split in their trunk center by a mirror symmetry plane. Fig. 2 shows a schematic representation of the calculation domain with a nucleus located at the bottom-left corner of the domain. The twin plane has been set as one domain boundary, in the present case the left yz plane, with a wetting angle condition imposed in a way similar to that of Sémoroz et al.(19) for dendrite growth in thin coatings. Instead of the condition $\vec{\nabla}\phi \cdot \vec{n_b} = 0$ (where $\vec{n_b}$ is the normal to the boundary) usually set for a symmetry plane, a condition $\vec{\nabla}\phi \cdot \vec{n_b} = -|\vec{\nabla}\phi| \cos\theta$ is imposed. For the sake of simplicity in the following, this boundary will be referred to as the twin plane. The wetting angle θ remains constant throughout the calculation and is measured within the solid, e.g., an angle larger than 90° corresponds to a grooved dendrite tip. A constant thermal gradient G is applied at an angle (α) with respect to the twin plane along the vertical y-axis. A constant cooling rate $\dot{T}$, is also imposed, thus allowing to update simply the temperature of each point of the domain at each time step (no heat equation is solved). Cell size was set to 0.1 μm.

Within this phase field approach, the artificially increased non-equilibrium effects associated with a thick solid-liquid interface have not been corrected yet. As the solute anti-trapping term developed by Echebarria et al (20), which scales with the interface thickness and solidification velocity, is not included in our formulation, the results only give qualitative trends but nevertheless point out interesting features of twinned dendrite growth. Typical properties of the alloy used for the modeling of twinned dendrite growth are shown in Table I.

Table I

Thermophysical Properties of an Al - 9 at. % Zn

D_s (m^2/s)	D_l (m^2/s)	Γ (K^{-1})	L_v (J/m^3)	k_0	T_m (°C)	m (°C)
1.16×10^{-13}	2.7×10^{-9}	2.3×10^{-7}	1×10^9	0.395	660	-357

This phase field model, already implemented succesfully in 2D in the Calcosoft®-PHF module, has been adapted up to 3D calculations using an explicit finite difference method (FDM) and a fixed orthogonal grid. The program has been written in order to be run on distributed

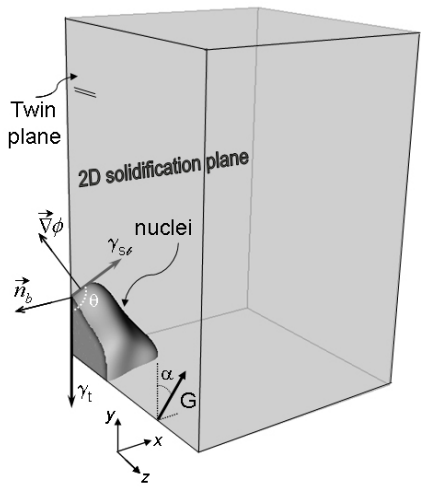

Figure 2: Calculation domain with the imposed thermal conditions and the Young-Laplace's equation imposed at the left yz boundary.

memory parallel machines. Thus, the 3D grid was divided in as many sub-grids as processors were to be involved in the calculation and the Message Passing Interface (MPI)(22) was used to exchange nodal values at the sub-grid boundaries. All calculations done in this work have been performed on a large cluster of AMD Opteron bi-processors at 2.4 Ghz with 4 Gbytes of memory each. Typically, 64 processors were used for 3D calculations of a $30 \times 60 \times 30$ μm^3 domain size.

Results and Discussion

In a first approach, the actual crystallographic growth direction of twinned dendrites has been supposed to be irrelevant for their tip shape and 2D simulations were performed in the xy plane of Fig. 2. A nucleus of a dendrite that should grow along $\langle 100 \rangle$ directions, i.e., $\epsilon_4 = 0.04$, $\epsilon_6 = \epsilon_8 = 0$ in eq. (4), was located at the bottom-left corner of a 2D domain. In this particular case, initial undercooling $\Delta T = 5\ K$, $G = 1 \times 10^5$ K/m and $\dot{T} = -100$ K/s, so the expected solidification speed v_s=$|\dot{T}|/G$ at steady-state is 1 mm/s. The G vector is perfectly aligned with the vertical axis ($\alpha = 0$). Fig. 3 shows the isovalue $\phi = 0.5$ in a 20×40 μm^2 domain, after 0.11 s for 4 different wetting conditions on the vertical-left twin boundary: $\theta = 90°$, $93°$, $95°$ and $100°$. Wetting on the bottom boundary corresponds to a standard symmetry condition $\theta = 90°$. Please note that this horizontal dendrite arm grows faster than the vertical one mainly because it is more undercooled with respect to the vertical thermal gradient. Although steady-state has not been reached in these simulations, it can be seen that the dendrite tip tends to grow away (split) from the twin plane when a wetting angle $\theta > 90°$ is imposed. As this angle is increased, tip splitting occurs earlier and, since the detached tip grows freely away from the boundary, it develops slightly faster. Such a behaviour has already been observed by Niederberger et al under isothermal conditions for a dendrite growing in thin coatings (21).

The extension of this situation to 3D is shown in Fig. 4b and can be compared with the 2D case of Fig. 4a obtained under identical conditions: $G = 1 \times 10^5$ K/m, $\Delta T = 5$ K, $\dot{T} = -70$ K/s and $\theta = 95°$. The solute concentration field after 0.06 s of growth is shown for the two cases with various gray levels (scale shown in the left). The view in Fig. 4b corresponds to the xy cut of the 3D result containing the dendrite tip and perpendicular to the twin plane.

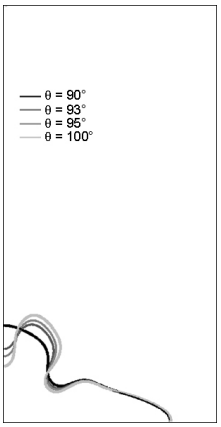

Figure 3: Effect of wetting angle on dendrite tip morphology in two dimensions. Dendrite tip splits earlier from the twin boundary as θ is increased. Domain is 20 x 40 μm^2, t = 0.011 s, $v_s = |\dot{T}|/G$= 1 mm/s, $\Delta T = 5$ K. The line contours represent the isovalues $\phi = 0.5$.

As solute rejection can occur also in the third dimension in 3D, the dendrite tip grows faster as compared with the 2D case. Associated consequences of this are: i) for the same wetting angle, the solid grows away (splits) from the twin boundary at an earlier stage in 3D; ii) the width of the liquid channel near the twin boundary, on the order of 0.5-2μm, depends on the depth of the groove and is reduced by about 25% when solute diffusion can occur also parallel to the twin boundary in 3D. The dendrite tip instantaneous velocity v^*, calculated from the length covered by the dendrite during $\Delta t = 0.005$ s, is 0.5 mm/s. It is still increasing at the time step shown in Fig. 4b, thus indicating that steady-state has not been yet achieved ($v_s = 0.7$ mm/s). From the composition field shown in this figure, the solute content in the liquid at the tip c_t^* (calculated from the average value of c and eq. 7 at $\phi = 0.5$) is only slightly lower than that exisiting at the bottom of the liquid channel c_d^*, e.g., $c_t^*/c_d^* = 0.984$. On the other hand, the extent of the liquid channel (21 μm) corresponds to a temperature difference of 2.1 K. Taking into acccount the curvature contribution of the tip (0.2 K) and neglecting that effect at the bottom of the doublon, this temperature difference can be converted into the correspondent compositions along the equilibrium liquidus line. One gets $c_t^*/c_d^* = 0.942$. The difference between these two ratios reveals the contribution of solute trapping, which is enhanced by the too large interface thickness used in our simulations.

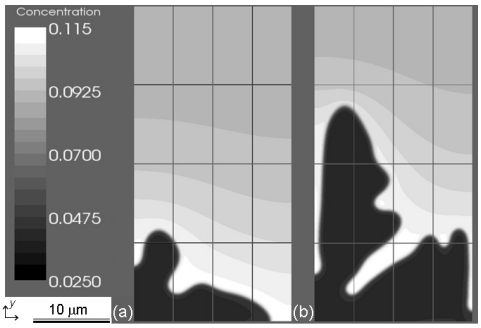

Figure 4: Solute concentration maps after 0.06 s of 2D (a) and 3D (b) $\langle 100 \rangle$ dendrites. Domain is 20 x 40 μm^2, $v_s = |\dot{T}|/G$= 0.7 mm/s, $\Delta T = 5$ K, $\theta = 95°$.

Finally, the effect of the direction of G was studied for dendrites growing along $\langle 110 \rangle$ directions. In this case $\epsilon_4 = \epsilon_8 = 0$ and $\epsilon_6 = -0.0172$ in eq. (4), $G = 1 \times 10^5$ K/m, $\Delta T = 4$ K, $\theta = 100°$ and $\dot{T} = -50$ K/m. In Fig. 5a and b, three dimensional views of a quart of these

dendrites are shown for $\alpha = 0°$ and 30°, respectively. The phase isosurface corresponds to $\phi = 0.5$ after 0.05 s of growth ($v_s = 0.5$ mm/s, $v^* = 0.18$ mm/s). The solid attached to the twin boundary can be clearly identified in the figure as black fields that lie within the corresponding yz twin boundary. It can be seen in Fig. 5a that the dendrite tip still grows away from the twin plane under the present conditions (reduced v_s, $\langle 110 \rangle$ growth). Even the in-plane $\langle 110 \rangle$ secondary arms also grow or split away from the twin boundary after some growth distance. However, when the direction of G is misoriented with respect to the vertical axis (Fig. 5b), the dendrite tip near the twin plane evolves at a higher undercooling and needs to grow faster ($v_s(\alpha = 30°)$= 0.58 mm/s, $v^* = 0.22$ mm/s). The depth of the liquid channel between the twin boundary and the dendrite arm aligned with the vertical axis evolves in a very similar way than that of a dendrite parallel to G, but the side arms parallel to the twin plane grow away from it at a later stage.

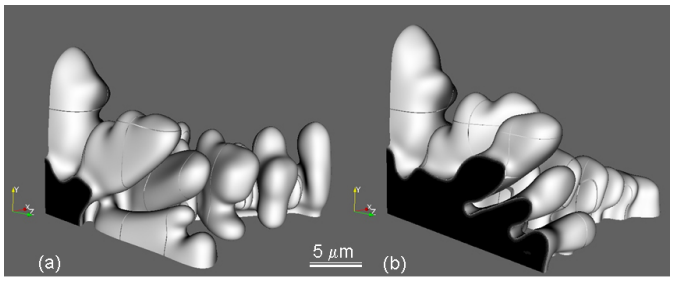

Figure 5: Effect of G with $\alpha = 0°$ (a) and 30° (b) from the vertical y-axis, on the $\langle 110 \rangle$ twinned dendrite morphology. The calculation domain was $30 \times 60 \times 30$ μm^3, but only the solidified region is shown. $v_s = |\dot{T}|/G$= 0.5 mm/s, $\Delta T = 4$ K, $\theta = 100°$.

In summary, it appears that as the Young-Laplace equation is satisfied at the twinned dendrite tip, it initiates a groove that degenerates quickly into a small doublon, regardless whether the calculations are 2D or 3D. For a fixed value of $\gamma_{s\ell}$, an increased twin boundary energy γ_t, i.e., an increased angle θ, tends to initiate the doublon at an earlier stage. The same occurs when diffusion in the liquid parallel to the twin plane is accounted for. The depth of the doublon does not seem to depend on the dendrite growth direction, providing it is aligned with the thermal gradient. The width of the doublon is very small and the associated segregation in this region seems to be less important than initially thought, i.e., the liquid pool composition at the deepest position of the liquid channel is smaller than c_0/k_0. Although this remains to be verified under steady state conditions when the anti-trapping correction will have been implemented, this reduced segregation is associated with liquid diffusion in the third dimension parallel to the twin plane. A narrow liquid channel with a reduced segregation could explain why experimental composition measurements near twinned dendrite trunks after complete solidification did not reveal an enhanced segregation compared to regular dendrites(6). Solid state diffusion perpendicular to the twin plane during cooling will further reduce any segregation revealing the presence of a doublon during growth.

Conclusion

Twinned dendrite tip morphology has been investigated through phase field modeling. Calculations have shown that, regardless of its value, a wetting angle imposed at the twin boundary promotes the formation of an apparent doublon dendrite shape. The thickness of the liquid

channel formed at the twin plane appears to be very narrow, thus quite difficult to elucidate experimentally. Moreover, the solute pile-up occurring in this region could be smeared out both by diffusion in the liquid parallel to the twin plane during solidification and subsequent solid state diffusion perpendicular to the twin plane during cooling. An extension of this work is presently being carried out in order to better understand twinned dendrite growth kinetics.

Acknowledgments

The authors thank the staff of the Mizar HPC facility at the Ecole Polytechnique Fédérale de Lausanne. The collaboration of Aurèle Mariaux and Jonas Valloton is also greatfully acknowledge.

References

[1] J.A. Eady and L.M. Hogan. J Cryst Growth, (1974), 129-136.

[2] H.J. Wood et al. Acta Mat, 45(2)(1997), 569-574.

[3] S. Henry. PhD thesis, Ecole Polytechnique Fédéral de Lausanne, (1999).

[4] J. Herenguel. Rev. Metall., 45(5)(1948),339-346.

[5] S. Henry et al. Acta Mater, 46(18)(1998), 2495-2501.

[6] M.A Salgado-Ordorica and M. Rappaz. Acta Mater 56(2008), 5708-5718

[7] S. Henry et al. Met and Mat Trans 35A(2004), 2495-2501.

[8] S.Z. Lu and J.D. Hunt. J Cryst Growth, 123(1992), 17-34.

[9] S. Liu et al. Acta Mater, 39(2001), 4271-4276.

[10] R.E. Napolitano and S. Liu. Phys Rev B, 70(2004), 214103.

[11] T. Haxhimali et al. Nature Materials, 5(2006), 660-664.

[12] M. Gündüz and J.D. Hunt. Acta metall, 37(7)(1989), 1839-1845.

[13] W.J. Boettinger et al. Annu. Rev. Mater. Res, 32(2002),163–194.

[14] J.C. Ramirez and C. Beckermann. Acta Mater, 53(2005), 1721-1736.

[15] C. Niederberger et al. Phys Rev E, 74(2006), 021604.

[16] A. Karma and W.-J. Rappel. Phys Rev E, 57(4)(1998), 4323-4349.

[17] W.R. Fehlner and S.H. Vosko. Can. J. Phys, 54(1976) 2159-2169.

[18] J. Tiaden et al. Phys D, 115(1998), 73-86.

[19] A. Sémoroz et al. Met and Mat Trans, 31A(2000), 487-495.

[20] B. Echebarria et Phys Rev E, 70(2004), 061604.

[21] C. Niederberger. PhD thesis, EPFL,(2007).

[22] M. Snir et al. MPI -The complete reference 1, The MPI Core, The MIT Press (1998)